

Schwinger pair production in counterpropagating laser pulses: Identifying volume factors

A. G. Tkachev,¹ I. A. Aleksandrov,^{1,2,*} and V. M. Shabaev^{1,3}

¹*Department of Physics, Saint Petersburg State University,
Universitetskaya Naberezhnaya 7/9, Saint Petersburg 199034, Russia*

²*Ioffe Institute, Politekhnicheskaya Street 26, Saint Petersburg 194021, Russia*

³*National Research Centre “Kurchatov Institute” B.P. Konstantinov Petersburg
Nuclear Physics Institute, Gatchina, Leningrad district 188300, Russia*

We investigate the nonperturbative process of vacuum pair production in a combination of two counterpropagating linearly polarized laser pulses of a finite spatial extent. By means of the locally-constant field approximation (LCFA), we calculate the total particle yield for the corresponding four-dimensional setup and compare it with the estimates obtained for simplified low-dimensional scenarios. Within the domain where the LCFA is well justified, we examine a combination of two plane-wave pulses, a standing electromagnetic wave, and a spatially uniform oscillating field and demonstrate that at each of these three levels of approximation, one can accurately predict the actual particle number by multiplying the results by properly chosen volume factors depending on the field parameters. We present closed-form expressions for these factors providing universal prescriptions for evaluating the particle yield. Our final formula connecting the spatially uniform setup with the four-dimensional scenario has a relative uncertainty of the level of 5%. The explicit correspondences deduced in this study not only prove the relevance of the approximate predictions, but also allow one to quickly estimate the number of pairs for various realistic scenarios without performing complicated numerical calculations.

I. INTRODUCTION

As became clear almost a century ago [1–3], a self-consistent theory of electromagnetic interactions can be formulated only within a many-particle approach permitting elementary processes with a nonconserving number of quanta, i.e., electrons e^- , positrons e^+ , and photons. In the presence of an external background field, these processes can manifest themselves in remarkable nonlinear phenomena which do not occur in classical Maxwell’s theory. One of the most staggering effects is the Sauter-Schwinger mechanism of vacuum electron-positron pair production in strong electromagnetic fields [1, 3, 4]. The probability of this process is generally suppressed by a small factor $\exp(-\pi E_c/E_0)$, where E_0 is the external electric field strength and $E_c = m^2 c^3 / |e\hbar| \sim 10^{16}$ V/cm is the so-called critical field strength (e and m are the electron charge and mass, respectively). This expression indicates that the pair-production mechanism is intrinsically nonperturbative with respect to E_0 , so by observing this phenomenon, one can probe the effects of quantum electrodynamics (QED) in strong fields in the regime where perturbation theory is no longer applicable.

The Sauter-Schwinger mechanism has not yet been investigated experimentally as its practical observation requires generation of superstrong electromagnetic backgrounds. One of the possible routes to measuring this effect relies on combining several intense laser pulses, which can become feasible in the near future due to a rapid development of the corresponding experimental tools (see recent reviews [5, 6]). Although very simple theoretical estimates can be obtained by means of the Schwinger formula discussed above, it is strongly desirable to accurately evaluate the number of e^+e^- pairs taking into account the spatiotemporal inhomogeneities of the

laser setup with the proper preexponential factor. The latter is, in fact, huge since the macroscopic laser fields are focused within the space-time region whose volume is much larger than $(\lambda/c)\lambda^3$, where $\lambda = \hbar/(mc)$ is the reduced Compton wavelength of the electron, which represents one of the natural scales in QED. Over the past decades, we have witnessed a substantial progress in the development of nonperturbative theoretical techniques, which allow one to describe the Sauter-Schwinger effect by means of various numerical approaches (see, e.g., Refs. [7–29]). Nevertheless, all of these methods can basically be employed for addressing quite simple low-dimensional scenarios which imply that the volume prefactor should be partially taken into account via manual multiplication of the numerical results by a proper dimensional number. For instance, a combination of two counterpropagating plane-wave laser pulses is infinite in the transverse plane, so the results should be multiplied by some effective area S . Moreover, we note that even within this simplified scenario, computing the number of pairs represents a very challenging task (see, e.g., Refs. [22, 30–33]).

The aim of the present study is to deduce the necessary volume factors allowing one to map the results of low-dimensional simulations onto the actual $(3 + 1)$ -dimensional setups. In particular, we will address the question of whether one can approximate a combination of two counterpropagating Gaussian laser pulses of a finite duration and spatial size by a uniform time-dependent electric background and then take into account the coordinate dependence by multiplying the results by a certain volume factor V (numerous theoretical studies were based on the corresponding so-called *dipole approximation* [8, 9, 12–17, 19, 21, 24–26, 28, 34–39]). Although the momentum distributions of particles are very sensitive to the spatiotemporal structure of the external field, we will demonstrate that the quantitative predictions of the *total* number of pairs can indeed be accurately obtained by properly choosing V and will provide simple analytical expressions for this volume factor. On the one hand, our findings will al-

* i.aleksandrov@spbu.ru

low one to easily obtain final numerical estimates for the total number of pairs. On the other hand, with the closed-form prescriptions for V , one will be able to avoid complicated and time-consuming calculations in the case of multidimensional inhomogeneities.

As we are interested in describing the nonperturbative Sauter-Schwinger effect of vacuum pair production, we assume that the external electromagnetic background is sufficiently strong and slowly varying. In this regime, our main theoretical tool will be the locally-constant field approximation (LCFA), where the total particle yield is computed by integrating the constant-field result over time and position space [40–50]. As will be shown below, the domain of the field parameters where the LCFA is well justified is very broad, so it covers many experimentally relevant field configurations.

Successively going from the dipole approximation (DA) to standing-wave and plane-wave approximations (SWA and PWA) and, finally, to the $(3 + 1)$ -dimensional setup, we will derive the volume factors connecting the corresponding scenarios. Combining then our results, we will provide a simple way to estimate the number of pairs produced in the most realistic field configuration by using only the rough DA predictions. It will be demonstrated that this procedure is quite universal to the choice of the laser-pulse profile and ensures the relative uncertainty of less than 5%.

The paper has the following structure. In Sec. II we describe the external field configuration involving two counter-propagating linearly polarized laser pulses and outline the approximate setups which appear within the PWA, SWA, and DA, respectively. In Sec. III we present the LCFA expressions for the total particle yield in each of the four scenarios. Section IV contains the main results of our study. Here we derive analytical formulas for the volume factors and assess their accuracy. Finally, we conclude in Sec. V.

Throughout the text, we employ the units $\hbar = c = 1$, $\alpha = e^2/(4\pi) \approx 1/137$.

II. EXTERNAL FIELD CONFIGURATIONS

A combination of two counterpropagating linearly polarized laser pulses will be described by the following expressions for the electric and magnetic field components:

$$\mathbf{E}(t, \mathbf{x}) = [\mathfrak{E}(\mathbf{x}, \omega t - \omega z) + \mathfrak{E}(\mathbf{x}, \omega t + \omega z)]\mathbf{e}_x, \quad (1)$$

$$\mathbf{H}(t, \mathbf{x}) = [\mathfrak{E}(\mathbf{x}, \omega t - \omega z) - \mathfrak{E}(\mathbf{x}, \omega t + \omega z)]\mathbf{e}_y, \quad (2)$$

where $\{\mathbf{e}_i\}$ are the unit vectors along the Cartesian axes, $\mathbf{x} = x\mathbf{e}_x + y\mathbf{e}_y + z\mathbf{e}_z$, $\mathfrak{E}(\mathbf{x}, \eta)$ describes an individual laser pulse, and ω is the corresponding carrier frequency. The most realistic field configuration within this study will involve two *Gaussian beams* of the following form:

$$\begin{aligned} \mathbf{E}^{(G)}(\mathbf{x}, \eta) &= \frac{E_0}{2} F(\eta) \frac{w_0}{w(z)} \exp\left[-\frac{x^2 + y^2}{w^2(z)}\right] \\ &\times \cos\left[\eta + \frac{\omega(x^2 + y^2)}{2R(z)} - \psi(z)\right], \end{aligned} \quad (3)$$

where

$$w(z) = w_0 \sqrt{1 + z^2/z_R^2}, \quad (4)$$

$$R(z) = z \left(1 + z_R^2/z^2\right), \quad (5)$$

$$\psi(z) = \arctan(z/z_R). \quad (6)$$

Here w_0 is the waist radius, $z_R = \pi w_0^2/\lambda$ is the Rayleigh range, and $\lambda = 2\pi/\omega$. The function $F(\eta)$ is a dimensionless smooth envelope function which vanishes for sufficiently large $|\eta|$. Within the paraxial approximation (3), we assume $w_0 \gg \lambda$, which is equivalent to the condition $\theta \ll 1$, where $\theta = \lambda/(\pi w_0)$ is the beam divergence. We will specify the corresponding setup $\mathbf{E}^{(G)}(t, \mathbf{x})$, $\mathbf{H}^{(G)}(t, \mathbf{x})$ by choosing the values of E_0 , ω , and w_0 . The interaction volume is governed by the length scales λ and w_0 .

In order to substantially simplify the structure of the external field, one can neglect the transverse coordinate dependence and set $w_0/w(z) = 1$, $\psi(z) = 0$. In this case, each Gaussian pulse turns into a plane electromagnetic wave which is infinite in the transverse x and y directions but still has a finite size along the z axis [22, 30–33]. Within this *plane-wave approximation* (PWA), the resulting external field reads

$$\begin{aligned} \mathbf{E}^{(PWA)}(t, z) &= \frac{E_0}{2} \left[F(\omega t - \omega z) \cos(\omega t - \omega z) \right. \\ &\quad \left. + F(\omega t + \omega z) \cos(\omega t + \omega z) \right] \mathbf{e}_x, \end{aligned} \quad (7)$$

$$\begin{aligned} \mathbf{H}^{(PWA)}(t, z) &= \frac{E_0}{2} \left[F(\omega t - \omega z) \cos(\omega t - \omega z) \right. \\ &\quad \left. - F(\omega t + \omega z) \cos(\omega t + \omega z) \right] \mathbf{e}_y. \end{aligned} \quad (8)$$

To further simplify the setup, one can completely disregard the spatial dependence of the envelope function, i.e., one can replace $F(\omega t \pm \omega z)$ with $F(\omega t)$. In this case, the external field will represent a standing electromagnetic wave, which is infinite in all of the spatial directions [18, 22, 27, 49, 51, 52]. The field configuration within the *standing-wave approximation* (SWA) has the following form:

$$\mathbf{E}^{(SWA)}(t, z) = E_0 F(\omega t) \cos \omega t \cos \omega z \mathbf{e}_x, \quad (9)$$

$$\mathbf{H}^{(SWA)}(t, z) = E_0 F(\omega t) \sin \omega t \sin \omega z \mathbf{e}_y. \quad (10)$$

Finally, one can approximate the external field by a spatially homogeneous background assuming that the particles are predominantly produced in the vicinity of the electric-field maxima. Here we set $z = 0$ and obtain

$$\mathbf{E}^{(DA)}(t) = E_0 F(\omega t) \cos \omega t \mathbf{e}_x, \quad (11)$$

$$\mathbf{H}^{(DA)}(t) = 0. \quad (12)$$

This approach will be called the *dipole approximation* (DA).

We underline that while the two Gaussian beams (G) are localized along each of the three spatial axes, the PWA setup is finite only with respect to the z axis and the SWA and DA fields are infinite along each of the three directions. This means that computing the number of e^+e^- pairs, one has to

take into account the corresponding volume factor depending on the approximation chosen. In what follows, we will identify these factors and provide simple prescriptions allowing one to map the results obtained for the four scenarios described above (DA \rightarrow SWA \rightarrow PWA \rightarrow G).

III. LOCALLY-CONSTANT FIELD APPROXIMATION

Here we will first present a general LCFA expression for the total number of pairs produced and then apply it to the specific field configurations described above.

A. General expression

The LCFA is based on the following closed-form expression for the total number of pairs produced per unit volume and time in the presence of a constant electromagnetic field [53]:

$$\frac{dN}{dt d\mathbf{x}} [\mathcal{E}, \mathcal{H}] = \frac{e^2 \mathcal{E} \mathcal{H}}{4\pi^2} \coth \frac{\pi \mathcal{H}}{\mathcal{E}} \exp\left(-\frac{\pi E_c}{\mathcal{E}}\right), \quad (13)$$

where

$$\mathcal{E} = \sqrt{\sqrt{\mathcal{F}^2 + \mathcal{G}^2} + \mathcal{F}}, \quad (14)$$

$$\mathcal{H} = \sqrt{\sqrt{\mathcal{F}^2 + \mathcal{G}^2} - \mathcal{F}}. \quad (15)$$

The Lorentz invariant quantities \mathcal{F} and \mathcal{G} are defined via $\mathcal{F} = (\mathbf{E}^2 - \mathbf{H}^2)/2$ and $\mathcal{G} = \mathbf{E} \cdot \mathbf{H}$.

Within the LCFA, one plugs the actual spatiotemporal dependence of the external inhomogeneous field into Eq. (13) and integrates it then over t and \mathbf{x} (see Refs. [40–50]):

$$N = \int d^4x \frac{dN}{dt d\mathbf{x}} [\mathcal{E}(\mathbf{x}), \mathcal{H}(\mathbf{x})], \quad (16)$$

where $\mathbf{x} = (t, \mathbf{x})$.

In the present study, the total number of particles will be evaluated by means of Eq. (16). Since the temporal and spatial variations of the external field are governed by the laser frequency ω , the LCFA is generally well justified once $(E_0/E_c)^{3/2} \gg \omega/m$ [49]. For a realistic laser wavelength of the order of 1 μm , this condition yields $E_0/E_c \gg 10^{-4}$. As will be shown below the pair production threshold in terms of the ratio E_0/E_c for this wavelength amounts to several hundredth, so we will be mainly focused on the interval $0.01 \leq E_0/E_c \leq 0.1$. Here the LCFA is definitely valid as even 0.01 is much larger than 10^{-4} . On the other hand, if we consider the minimal value $E_0 = 0.01 E_c$ used in our calculations, then the laser frequency and wavelength will have to satisfy $\omega/m \ll 10^{-3}$ and $\lambda \gg 4 \times 10^{-4} \mu\text{m}$, respectively, which is completely realistic.

B. Dipole approximation (DA)

If the external field does not depend on the spatial coordinates, then Eq. (16) takes the following simple form:

$$\frac{N^{(\text{DA})}}{V} = \frac{e^2}{4\pi^3} \int_{-\infty}^{+\infty} dt E^2(t) \exp\left[-\frac{\pi E_c}{|E(t)|}\right], \quad (17)$$

where $V = \int d\mathbf{x}$ is the normalization volume and $E(t)$ is the corresponding electric field strength. In our case,

$$E(t) = E_0 F(\omega t) \cos \omega t. \quad (18)$$

Since the field depends on t via the product ωt , one can substitute $\eta = \omega t$ in Eq. (17) and immediately reveal that the right-hand side is inversely proportional to ω . Accordingly, we will discuss the results in terms of the following dimensionless ω -independent quantity:

$$\nu^{(\text{DA})} = \frac{\omega N^{(\text{DA})}}{m^4 V}. \quad (19)$$

Its explicit form is given by

$$\nu^{(\text{DA})} = \frac{1}{4\pi^3} \frac{E_0^2}{E_c^2} \int_{-\infty}^{+\infty} d\eta f^2(\eta) \exp\left[-\frac{\pi E_c}{E_0 |f(\eta)|}\right], \quad (20)$$

where

$$f(\eta) = F(\eta) \cos \eta. \quad (21)$$

C. Standing-wave approximation (SWA)

Here we again factor out the ω dependence:

$$\nu^{(\text{SWA})} = \frac{\omega N^{(\text{SWA})}}{m^4 V}. \quad (22)$$

Let us introduce the following ω -independent function representing a Lorentz invariant:

$$\mathcal{F}(\eta, \xi) = \frac{1}{2} \left\{ [\mathbf{E}^{(\text{SWA})}(\eta/\omega, \xi/\omega)]^2 - [\mathbf{H}^{(\text{SWA})}(\eta/\omega, \xi/\omega)]^2 \right\}. \quad (23)$$

Taking into account Eqs. (9) and (10), one obtains

$$\mathcal{F}(\eta, \xi) = \frac{E_0^2}{2} F^2(\eta) \cos(\eta + \xi) \cos(\eta - \xi). \quad (24)$$

Then we will calculate

$$\begin{aligned} \nu^{(\text{SWA})} &= \frac{1}{4\pi^4} \int_{-\infty}^{+\infty} d\eta \int_{-\pi}^{\pi} d\xi \theta(\mathcal{F}(\eta, \xi)) \\ &\times \frac{\mathcal{F}(\eta, \xi)}{E_c^2} \exp\left[-\frac{\pi E_c}{\sqrt{2\mathcal{F}(\eta, \xi)}}\right]. \end{aligned} \quad (25)$$

Here the Heaviside step function θ indicates that e^+e^- pairs are generated only in the space-time regions where the electric field is stronger than the magnetic component. If the latter is not the case, one can Lorentz transform the external field, so that it becomes purely magnetic and, thus, does not produce pairs.

D. Plane-wave approximation (PWA)

Since the external field is now finite along the z axis, the total number of particles per unit transverse cross sectional area S is also finite. We will compute the following quantity:

$$\nu^{(\text{PWA})} = \frac{\omega^2 N^{(\text{PWA})}}{m^4 S}. \quad (26)$$

It also does not depend on ω . Here it is convenient to introduce $\eta_- = \omega(t - z)$ and $\eta_+ = \omega(t + z)$. We find

$$\begin{aligned} \nu^{(\text{PWA})} &= \frac{1}{8\pi^3} \frac{E_0^2}{E_c^2} \int_{-\infty}^{+\infty} d\eta_- \int_{-\infty}^{+\infty} d\eta_+ \theta(f(\eta_-)f(\eta_+)) \\ &\times f(\eta_-)f(\eta_+) \exp\left[-\frac{\pi E_c}{E_0 \sqrt{f(\eta_-)f(\eta_+)}}\right], \end{aligned} \quad (27)$$

where $f(\eta)$ is defined in Eq. (21).

E. Gaussian beams (G)

The invariant \mathcal{F} is now given by

$$\mathcal{F} = 2\mathfrak{E}(\mathbf{x}, \omega t - \omega z)\mathfrak{E}(\mathbf{x}, \omega t + \omega z). \quad (28)$$

Let us introduce

$$g(\mathbf{x}, \eta) = F(\eta) \cos\left[\eta + \frac{\omega(x^2 + y^2)}{2R(z)} - \psi(z)\right]. \quad (29)$$

Then

$$\begin{aligned} \mathcal{F} &= \frac{E_0^2}{2} \frac{w_0^2}{w^2(z)} \exp\left[-\frac{2(x^2 + y^2)}{w^2(z)}\right] \\ &\times g(\mathbf{x}, \omega t - \omega z)g(\mathbf{x}, \omega t + \omega z). \end{aligned} \quad (30)$$

In order to calculate the total number of pairs N according to Eq. (16), we again introduce $\eta_{\pm} = \omega(t \pm z)$ and also rescale the variables x and y as $x = w_0\rho_x$, $y = w_0\rho_y$. Since $z = (\eta_+ - \eta_-)/(2\omega)$, we represent $w(z)$ as

$$w(z) = w_0\rho(\eta_+ - \eta_-), \quad (31)$$

where

$$\rho(\eta) = \sqrt{1 + \frac{\eta^2}{4\omega^2 z_R^2}} = \sqrt{1 + \left(\frac{\eta}{\omega^2 w_0^2}\right)^2}. \quad (32)$$

We now obtain

$$\begin{aligned} N^{(\text{G})} &= \frac{1}{8\pi^3} \frac{m^4 E_0^2}{\omega^4 E_c^2} (\omega w_0)^2 \int d\rho_x d\rho_y d\eta_- d\eta_+ \\ &\times \theta(g(\mathbf{x}, \eta_-)g(\mathbf{x}, \eta_+)) \frac{1}{\rho^2(\eta_+ - \eta_-)} \\ &\times \exp\left[-\frac{2(\rho_x^2 + \rho_y^2)}{\rho^2(\eta_+ - \eta_-)}\right] g(\mathbf{x}, \eta_-)g(\mathbf{x}, \eta_+) \\ &\times \exp\left\{-\frac{\pi E_c}{E_0} \rho(\eta_+ - \eta_-) \exp\left[\frac{\rho_x^2 + \rho_y^2}{\rho^2(\eta_+ - \eta_-)}\right]\right\} \\ &\times \frac{1}{\sqrt{g(\mathbf{x}, \eta_-)g(\mathbf{x}, \eta_+)}} \}, \end{aligned} \quad (33)$$

where in the functions $g(\mathbf{x}, \eta_{\pm})$ we imply $x = w_0\rho_x$, $y = w_0\rho_y$, and $z = (\eta_+ - \eta_-)/(2\omega)$. Finally, we employ polar coordinates in the $\rho_x\rho_y$ plane, integrate over the polar angle, and substitute $\chi = \rho^2$, where ρ is the corresponding radius, $\rho = \sqrt{\rho_x^2 + \rho_y^2}$. This brings us to the following final expression:

$$\begin{aligned} N^{(\text{G})} &= \frac{1}{8\pi^2} \frac{m^4 E_0^2}{\omega^4 E_c^2} (\omega w_0)^2 \int_0^{+\infty} d\chi \int_{-\infty}^{+\infty} d\eta_- \int_{-\infty}^{+\infty} d\eta_+ \\ &\times \theta(\tilde{g}(\chi, z, \eta_-)\tilde{g}(\chi, z, \eta_+)) \frac{1}{\rho^2(\eta_+ - \eta_-)} \\ &\times \exp\left[-\frac{2\chi}{\rho^2(\eta_+ - \eta_-)}\right] \tilde{g}(\chi, z, \eta_-)\tilde{g}(\chi, z, \eta_+) \\ &\times \exp\left\{-\frac{\pi E_c}{E_0} \rho(\eta_+ - \eta_-) \exp\left[\frac{\chi}{\rho^2(\eta_+ - \eta_-)}\right]\right\} \\ &\times \frac{1}{\sqrt{\tilde{g}(\chi, z, \eta_-)\tilde{g}(\chi, z, \eta_+)}} \}, \end{aligned} \quad (34)$$

where

$$\tilde{g}(\chi, z, \eta) \equiv F(\eta) \cos\left[\eta + \frac{\omega w_0^2 \chi}{2R(z)} - \psi(z)\right] \quad (35)$$

and $z = (\eta_+ - \eta_-)/(2\omega)$.

Here the result is finite and depends on the field parameters E_0 , ω , and w_0 . Nevertheless, as can be easily seen, the integrand in Eq. (34) involves only E_0 and the product $\omega w_0 = 2/\theta$, so it is convenient to define

$$\nu^{(\text{G})} = \frac{\omega^4}{m^4} N^{(\text{G})}, \quad (36)$$

which depends only on E_0 and θ . As was mentioned above, the paraxial approximation is valid for sufficiently small values of θ , i.e., large ωw_0 .

IV. RESULTS

Here we will numerically evaluate Eqs. (20), (25), (27), and (34). By comparing the results of the different approximations, we aim at deriving simple closed-form expressions that establish the corresponding relations among them. In our numerical calculations, we employ the Gaussian envelope

$$F(\eta) = e^{-(\eta/\sigma)^2}, \quad (37)$$

where σ is a dimensionless parameter governing the laser pulse duration.

In what follows, we will separately discuss the transitions DA \rightarrow SWA, SWA \rightarrow PWA, and PWA \rightarrow G.

A. SWA versus DA

According to our numerical results, the DA always overestimates the particle yield, which is no surprise as this approx-

imation neglects the spatial profile of the external field by replacing it with unity and, thus, notably increases the local values of the field strength. Within the SWA, the particles are primarily produced in the vicinity of the maxima of the standing-wave electric component. Let us consider $z \sim 0$ in Eq. (9) and identify the vicinity $(-\delta, \delta)$ providing the dominant contribution to the particle number within the corresponding cycle of the cosine profile. According to Eq. (13), we suggest using the following relation:

$$\cos^2 \omega \delta \exp\left(-\frac{\pi E_c}{E_0 \cos \omega \delta}\right) = \zeta \exp\left(-\frac{\pi E_c}{E_0}\right), \quad (38)$$

which indicates that the particle density $dN/(dtdx)$ at $z = \delta$ equals its value at $z = 0$ multiplied by a small number ζ . The latter will be determined by fitting our numerical results. Equation (38) can be solved numerically yielding the function $\delta = \delta_\zeta(E_0)$. The corresponding ‘‘reduction factor’’ is found then via

$$D_\zeta(E_0) = \frac{2\delta}{(2\pi/\omega)} = \frac{\omega\delta}{\pi}. \quad (39)$$

The crucial question here is whether one can find a *universal* value of ζ , so that $\nu^{(\text{SWA})}/\nu^{(\text{DA})} \approx D_\zeta(E_0)$ for all E_0 . By calculating the ratio $\nu^{(\text{SWA})}/\nu^{(\text{DA})}$ numerically, we will identify ζ which generates the most accurate approximation $D_\zeta(E_0)$. In the weak field limit $E_0 \ll E_c$, the preexponential factor $\cos^2 \omega \delta$ in Eq. (38) can be replaced with unity. In this case, one obtains a simple closed-form solution

$$D_\zeta^{(0)}(E_0) = \frac{1}{\pi} \arccos \frac{1}{1 - \frac{E_0}{\pi E_c} \ln \zeta}. \quad (40)$$

In Fig. 1 we depict the exact ratio $\nu^{(\text{SWA})}/\nu^{(\text{DA})}$ computed numerically and the functions $D_\zeta(E_0)$ and $D_\zeta^{(0)}(E_0)$ for $\zeta = 0.044$. By exact values we mean those obtained directly by the LCFA expressions (20) and (25). We observe that the approximate reduction factor $D_\zeta(E_0)$ provides indeed a very accurate prescription for estimating $\nu^{(\text{SWA})}$ by means of $\nu^{(\text{DA})}$. Here we employed $\sigma = 5$, while, according to our results, the ratio displayed in Fig. 1 is almost independent of the pulse duration (for $\sigma \gtrsim 3$, the curves would be completely indistinguishable in the plot; the curve for $\sigma = 1$ would deviate from that displayed in Fig. 1 only for $E_0 \gtrsim E_c$). On the other hand, the quantities $\nu^{(\text{DA})}$ and $\nu^{(\text{SWA})}$ themselves notably depend on σ at any E_0 . This suggests that our prescription is indeed quite universal. The leading-order estimate $D_\zeta^{(0)}(E_0)$ [Eq. (40)] can be utilized for $E_0 \lesssim 0.1E_c$, so it represents a very useful expression in the realistic domain of subcritical fields. We also point out that, e.g., within the interval $0.01E_c \leq E_0 \leq 0.1E_c$, the quantities $\nu^{(\text{DA})}$ and $\nu^{(\text{SWA})}$ vary over a huge region covering many orders of magnitude (for $E_0 = 0.01E_c$ and $\sigma = 5$ we obtain $\nu^{(\text{DA})} \approx 4 \times 10^{-144}$, while for $E_0 = 0.1E_c$ we have $\nu^{(\text{DA})} \approx 8 \times 10^{-19}$).

The analysis performed in this section provides also additional insights concerning the validity of the LCFA. The condition $(E_0/E_c)^{3/2} \gg \omega/m$ discussed above is equivalent to the requirement that the effective vicinity δ be much larger

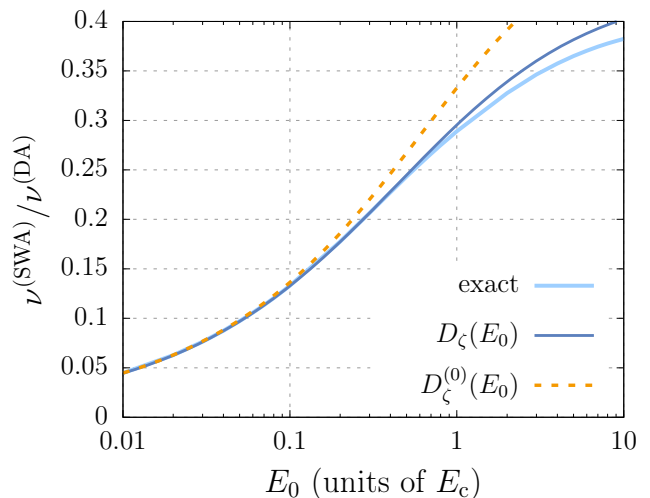


Figure 1. Ratio $\nu^{(\text{SWA})}/\nu^{(\text{DA})}$ evaluated via Eqs. (20) and (25) for $\sigma = 5$ (‘‘exact’’) and the functions $D_\zeta(E_0)$ and $D_\zeta^{(0)}(E_0)$ for $\zeta = 0.044$.

than the pair formation length $m/|eE_0|$. This is equivalent to $D_\zeta(E_0) \gg \gamma$, where $\gamma = m\omega/|eE_0|$ is the Keldysh parameter characterizing the laser field. For a realistic laser wavelength of $1 \mu\text{m}$ and $E_0 > 0.01E_c$, we obtain $\gamma < 3.9 \times 10^{-5}$, which definitely ensures $\gamma \ll D_\zeta(E_0)$ since $D_\zeta(E_0) \gtrsim 0.05$ according to Fig. 1.

B. PWA versus SWA

Our goal here is to take into account the finiteness of the laser pulses, which is neglected within the SWA. The total number of pairs $N^{(\text{PWA})}$ obtained within the PWA is proportional to the cross sectional area S , while $N^{(\text{SWA})}$ contains the volume $V = LS$. It is necessary to construct the effective length L as a function of the field parameters. It is natural to represent it as $L = (2\pi/\omega)N_{\text{eff}}$, where N_{eff} is a dimensionless quantity, which can be viewed as an effective number of cycles in the laser pulse. From Eqs. (22) and (26), it follows that the condition $N^{(\text{PWA})} = N^{(\text{SWA})}$ is equivalent to

$$\frac{\nu^{(\text{PWA})}}{\nu^{(\text{SWA})}} = 2\pi N_{\text{eff}}. \quad (41)$$

In the realistic subcritical domain $E_0 \lesssim 0.1E_c$ and quasistatic regime under consideration, the presence of the Gaussian envelope (37) makes the pair-production process efficiently occur only within *one* carrier cycle in the vicinity of the field maximum [$\eta = 0$ in Eq. (37)]. Since within the PWA the laser pulses do not fully overlap, one may expect that the correct estimate is $N_{\text{eff}} \approx 1/2$, so

$$\frac{\nu^{(\text{PWA})}}{\nu^{(\text{SWA})}} \approx \pi. \quad (42)$$

According to our calculations, this is indeed a quite accurate relation once $E_0 \ll E_c$. However, it can be significantly improved.

First, let us take into account that in the vicinity of the field maximum $\eta = \xi = 0$ in Eq. (25) or $\eta_- = \eta_+ = 0$ in Eq. (27), the spatial profile of the laser pulses in the PWA is not governed solely by the cosine but also involves the envelope. At $\eta = \omega t = 0$, the field profile in the exponential function in Eq. (27) as a function of $\xi = \omega z$ reads $F(\xi) \cos \xi$, which yields

$$F(\xi) \cos \xi = 1 - \left(\frac{1}{2} + \frac{1}{\sigma^2} \right) \xi^2 + \mathcal{O}(\xi^4). \quad (43)$$

We observe that the field shape depends on σ via the envelope function, which alters the effective length L and, thus, the ratio (41). Equation (43) suggests that L is proportional to $(1/2 + 1/\sigma^2)^{-1/2}$, i.e., to $(1 + 2/\sigma^2)^{-1/2}$. Although the estimate (42) is correct in the limit $\sigma \gg 1$, for relatively small values of σ , it should be modified according to

$$\frac{\nu^{(\text{PWA})}}{\nu^{(\text{SWA})}} \approx \frac{\pi}{\sqrt{1 + 2/\sigma^2}}. \quad (44)$$

This modification is irrelevant for $\sigma \gg 1$, whereas for small σ it notably increases the accuracy of our prescription.

Although Eq. (44) is already quite precise for $E_0 \ll E_c$, our calculations reveal that the ratio $\nu^{(\text{PWA})}/\nu^{(\text{SWA})}$ also depends on E_0 , which becomes important for $E_0 \sim 0.1E_c$ (this ratio cannot involve ω as was pointed out in Sec. III). For larger values of E_0 and σ , the e^+e^- pairs can also be produced at other local maxima of the external field. For instance, one can also consider the vicinity of $\xi = \pi$ in Eq. (43). In this case, the external field is suppressed by the envelope factor $\exp[-(\pi/\sigma)^2]$, which has a great impact on the Schwinger exponential in, e.g., Eq. (27). Replacing E_0 with $E_0 \exp[-(\pi/\sigma)^2]$ in this exponent is equivalent to raising the latter to the power of $\exp[(\pi/\sigma)^2]$, so we propose the following correction:

$$\nu^{(\text{PWA})} \approx \frac{\pi}{\sqrt{1 + 2/\sigma^2}} \nu^{(\text{SWA})} + 2[\pi \nu^{(\text{SWA})}]^{\exp[(\pi/\sigma)^2]}. \quad (45)$$

The factor of 2 in the last term appears due to the analogous contribution from $\xi = -\pi$. We will use Eq. (45) as our final prescription and examine its accuracy.

Our simple analysis of the pulse shape effects must be justified by direct numerical computations and prove to be universal with respect to the changes of the field parameters. In Fig. 2(a) we display the exact ratio $\nu^{(\text{PWA})}/\nu^{(\text{SWA})}$ calculated via Eqs. (25) and (27) and the estimate (45) as a function of E_0 (note the shift of the origin of the plot). We observe that for large σ the ratio $\nu^{(\text{PWA})}/\nu^{(\text{SWA})}$ becomes indeed rather sensitive to E_0 , which can be approximately taken into account by means of the second term in Eq. (45). On the other hand, for $E_0 \ll E_c$ the first term in Eq. (45) very accurately reproduces the exact ratio. In Fig. 2(b) we present the relative uncertainty of Eq. (45). The error increases with E_0 and σ , but does not exceed 10% for the parameters employed in our calculations. Here we refrain from the analysis of larger values of E_0 since in this case one has to incorporate contributions from $\xi = \pm 2\pi$, which complicates the formulas, while the

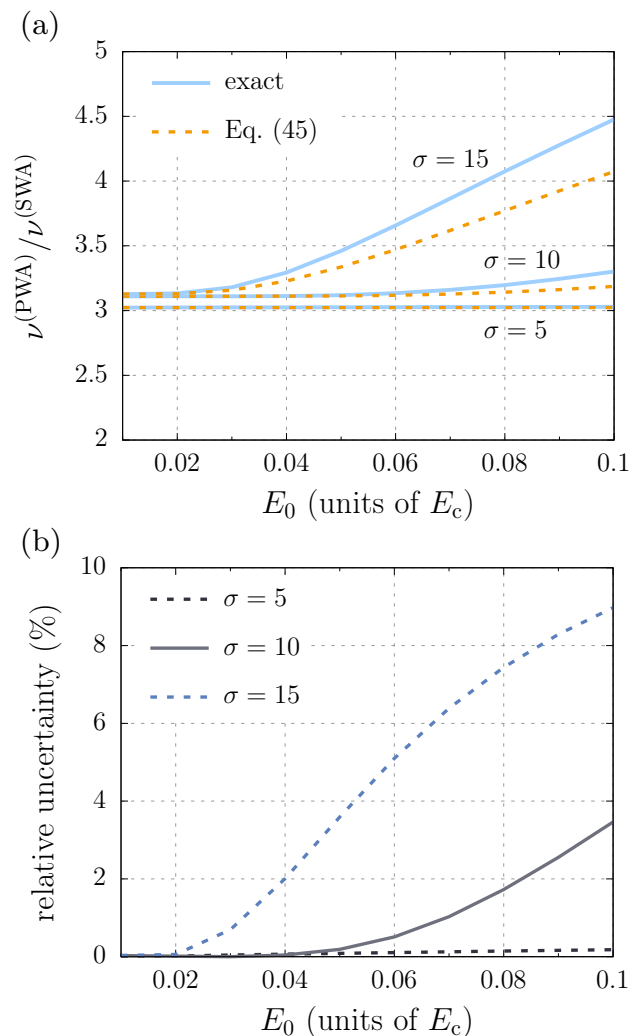


Figure 2. (a) Ratio $\nu^{(\text{PWA})}/\nu^{(\text{SWA})}$ evaluated via Eqs. (25) and (27) (solid lines) and obtained by means of the approximate prescription (45) (dashed lines). In the Gaussian envelope (37), we use $\sigma = 5, 10$, and 15 . (b) Relative uncertainty of Eq. (45) as a function of E_0 for various values of σ .

domain $E_0 \gtrsim 0.1E_c$ appears to be much less relevant from the experimental viewpoint (as will be shown in Sec. IV D, the actual pair production threshold is below $0.1E_c$).

C. Gaussian beams versus PWA

Now our goal is to incorporate the transverse structure of the laser pulses. Note that Eqs. (26) and (36) lead to the following relation:

$$\frac{\nu^{(\text{G})}}{\nu^{(\text{PWA})}} = \omega^2 S, \quad (46)$$

where we have assumed $N^{(\text{G})} = N^{(\text{PWA})}$. To estimate the effective area S , we first point out that it should be proportional to ω_0^2 , which is clear from the analysis of dimen-

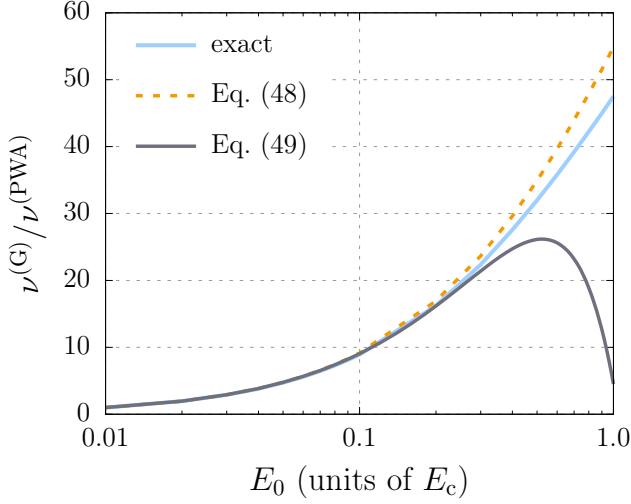


Figure 3. Ratio $\nu^{(G)}/\nu^{(PWA)}$ evaluated via Eqs. (27) and (34) (solid light blue line) and obtained by means of the approximate expressions (48) (dashed line) and (49) (solid dark gray line). The field parameters are $\sigma = 5$ and $\omega w_0 = 10$.

sions. This is also in agreement with the fact that $\nu^{(PWA)}$ is ω -independent, while $\nu^{(G)}$ depends only on the product $\omega w_0 = 2/\theta$. Accordingly, the right-hand side of Eq. (46) should read $(\omega w_0)^2 h(E_0/E_c, \sigma)$, where the function h is to be determined.

The pulse duration σ governs the longitudinal structure of the laser field, so the function $h(E_0/E_c, \sigma)$ is, in fact, almost insensitive to σ . On the other hand, the field amplitude E_0 strongly affects the volume factor. Its qualitative behavior in the limit $E_0 \ll E_c$ can be identified by inspecting the Schwinger exponential $\exp(-\pi E_c/E_0)$, where E_0 is modified by the factor $e^{-\chi}$ [see Eq. (34)]. The effective radius of the vicinity of $x = y = 0$ ($\chi = 0$) will possess the same scaling with respect to E_0 as δ in Eq. (39), i.e., it will be proportional to $\sqrt{E_0/E_c}$ for $E_0 \ll E_c$, which follows from Eq. (40). Therefore, the effective area is linear in E_0 :

$$\frac{\nu^{(G)}}{\nu^{(PWA)}} \approx A(\omega w_0)^2 \frac{E_0}{E_c} \quad (47)$$

for $E_0 \ll E_c$. It turns out that by carefully inspecting Eq. (34), one can extract the constant A and also derive an approximate expression valid up to $E_0 \sim E_c$ (see the Appendix). The result reads

$$\frac{\nu^{(G)}}{\nu^{(PWA)}} \approx \frac{\pi}{2} (\omega w_0)^2 \left[1 - \frac{\pi E_c}{E_0} - \left(\frac{\pi E_c}{E_0} \right)^2 e^{\pi E_c/E_0} \text{Ei} \left(-\frac{\pi E_c}{E_0} \right) \right], \quad (48)$$

where $\text{Ei}(z)$ is the exponential integral. In the limit $E_0 \ll E_c$, this expression yields

$$\frac{\nu^{(G)}}{\nu^{(PWA)}} \approx (\omega w_0)^2 \frac{E_0}{E_c} \left(1 - \frac{3 E_0}{\pi E_c} \right). \quad (49)$$

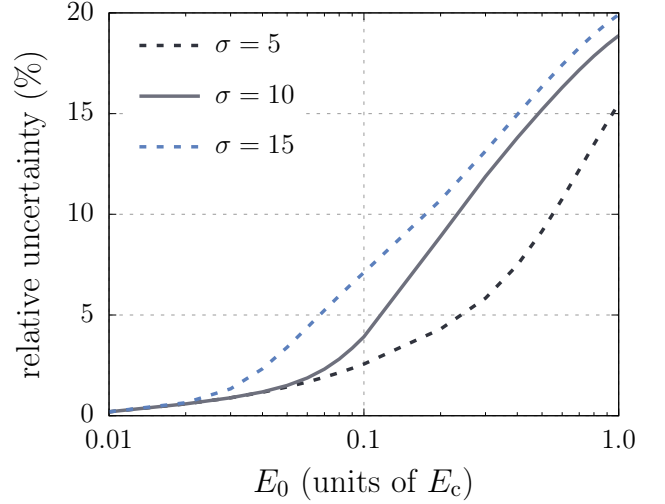


Figure 4. Relative uncertainty of Eq. (48) as a function of E_0 for various values of σ ($\omega w_0 = 10$).

It turns out that this expansion already provides a very accurate prescription within the subcritical domain $0.01E_c \leq E_0 \leq 0.1E_c$.

In Fig. 3 we present the ratio $\nu^{(G)}/\nu^{(PWA)}$ calculated directly via Eqs. (27) and (34) and by means of the approximate formulas (48) and (49) for $\sigma = 5$ and $\omega w_0 = 10$. First, we observe that in the region $E_0 \lesssim 0.1E_c$, both approximations (48) and (49) are quite precise. For $E_0 \gtrsim 0.1E_c$ the all-order expression (48) still provides rather accurate predictions although the corresponding uncertainty grows with increasing E_0 . For larger values of the field strength E_0 , the spatiotemporal domain where the field produces pairs expands, so it generally becomes more difficult to take into account the field inhomogeneities. Second, our numerical results indicate that the curves displayed in Fig. 3 are visually indistinguishable from the analogous results for different ωw_0 , provided they are trivially rescaled by the factor $(\omega w_0)^2$ (we performed the calculations for $5 \leq \omega w_0 \leq 50$). Nevertheless, the exact ratio $\nu^{(G)}/\nu^{(PWA)}$ is rather sensitive to σ and so is the quality of the approximations (48) and (49), which are σ -independent. In Fig. 4 we display the relative uncertainty of Eq. (48) versus E_0 for several different σ . Since we focus on the regime $0.01E_c \leq E_0 \leq 0.1E_c$, we conclude that Eq. (48) ensures the uncertainty of less than 10% for $\sigma \leq 20$. Furthermore, for $E_0 \leq 0.1E_c$ one can employ the simpler expression (49), which has the same quality as Eq. (48).

D. From DA to Gaussian beams

Combining Eqs. (36), (40), (45), and (49), we obtain the final expression:

$$\begin{aligned}
 N^{(G)} &= \frac{m^4 w_0^2 E_0}{\omega^2 E_c} \left(1 - \frac{3 E_0}{\pi E_c} \right) \\
 &\times \left\{ \frac{\nu^{(DA)}}{\sqrt{1+2/\sigma^2}} \arccos \left(1 + \frac{E_0}{E_c} \right)^{-1} \right. \\
 &\left. + 2 \left[\nu^{(DA)} \arccos \left(1 + \frac{E_0}{E_c} \right)^{-1} \right] e^{(\pi/\sigma)^2} \right\}, \quad (50)
 \end{aligned}$$

where $\ln \zeta = \ln 0.044 = -3.12$ was replaced with $-\pi$. The formula (50) represents the main result of our study. It allows one to obtain the total number of electron-positron pairs produced in the complex $(3+1)$ -dimensional setup involving finite Gaussian laser pulses having in hand only the results obtained for the simplest spatially uniform field configuration (11).

To demonstrate the robustness of our prescription, we analyze the relative uncertainty of Eq. (50) for various σ and E_0 (see Fig. 5). Since Eq. (50) is a composition of three mappings, it is no surprise that its accuracy nontrivially depends on the variables E_0 and σ . For instance, for $\sigma = 15$ and $\sigma = 20$, Eq. (50) is extremely accurate as it provides the results with an error of less than 2% although at each intermediate step in Secs. IV A, IV B, and IV C, our approximations were less precise. The reason for this behavior is that Eqs. (40) and (49) basically overestimate the results, whereas Eq. (45) underestimates them. Although we expected the overall uncertainty of the level of 10%, according to Fig. 5, it proves to be always less than 5%, which allows one to obtain even more accurate predictions. We point out that the error does not exceed 3% also in the case of ultrashort pulses with $\sigma = 1$ and is almost insensitive to ωw_0 . According to our numerical analysis, the prescription (50) is also universal with respect to the envelope shape of the laser pulses. We directly made sure that the relative uncertainty remains the same also for $F(\eta) = 1/\cosh^2(\eta/\sigma)$.

Let us now provide an explicit numerical example. Suppose we are interested in estimating the total number of pairs for the setup involving two counterpropagating Gaussian pulses with the following parameters: $E_0 = 0.07E_c$, $\sigma = 5$, $\omega w_0 = 10$ (divergence $\theta = 0.2$). By evaluating Eq. (20), we find $\nu^{(DA)} = 4.44 \times 10^{-25}$. Then by means of Eq. (50), in terms of $\nu^{(G)} = (\omega/m)^4 N^{(G)}$ we obtain $\nu^{(G)} = 1.01 \times 10^{-24}$. It is very close to the value obtained via Eq. (34), which amounts to $\nu^{(G)} = 9.83 \times 10^{-25}$ (the uncertainty is 3.3%). To obtain the total number of electron-positron pairs, one has to multiply $\nu^{(G)}$ by a factor of $(m/\omega)^4$, which governs the 4-volume of the interaction region and represents a huge number since ω is basically several orders of magnitude smaller than m in realistic scenarios. For instance, if the laser wavelength is $1 \mu\text{m}$, then $\omega/m = 3.86 \times 10^{-7}$ and $(m/\omega)^4 = 4.50 \times 10^{25}$. In this case, we obtain 46(2) pairs. Our numerical results also yield an accurate estimate for the pair production threshold. It turns out that to observe the Schwinger effect, it is already

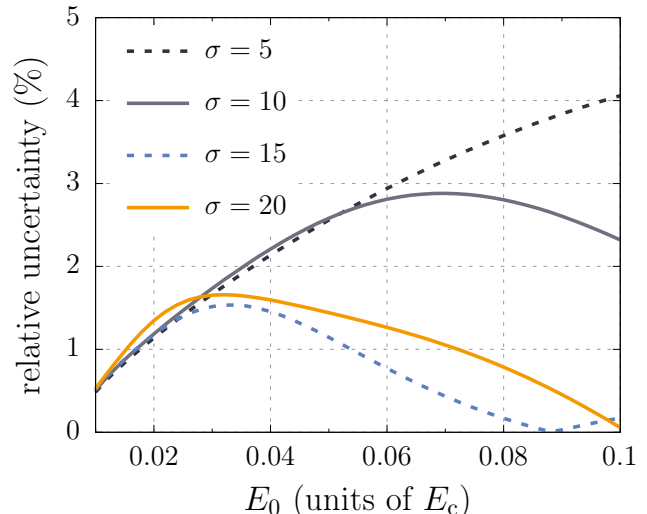


Figure 5. Relative uncertainty of the final prescription (50) as a function of E_0 for various values of σ ($\omega w_0 = 10$).

sufficient to generate two laser pulses with a resulting amplitude of $0.07E_c$, which is one order of magnitude smaller than the critical value E_c and corresponds to the peak intensity of $5.7 \times 10^{26} \text{ W/cm}^2$ for each of the two coherent laser pulses. This value is in agreement with Refs. [42, 43], where a different model of counterpropagating laser pulses was investigated. The pair production threshold can be, in principle, lowered due to dynamical effects [54–56] or by focusing a larger number of laser beams [46].

V. CONCLUSION

In this study, we deduced simple analytical expressions connecting numerical results for the total particle yield within various approaches to modelling the external field of two counterpropagating laser pulses. Although the existence of an explicit correspondence between the dipole approximation and $(3+1)$ -dimensional scenario is nontrivial itself, we derived a universal formula which ensures a relative uncertainty of less than 5%. It clearly indicates that the information on the total number of pairs produced by Gaussian beams is already encoded in the simplest setup depending solely on time. It turns out that the envelope function and the oscillating carrier incorporated in the dipole approximation provide one with the necessary estimates, so one should only map them onto the more involved scenario according to the prescription presented in this study. We underline here that the simplified spatially homogeneous setup completely fails to describe the actual momentum distributions of the particles as it disregards the nontrivial dynamics of the created electrons and positrons in the external inhomogeneous background field.

The explicit formulas for the volume factors identified in the present study are expected to be particularly useful for experimentalists as these expressions allow one to easily estimate the particle yield and do not require complicated nu-

merical procedures. Finally, we demonstrated that the actual pair production threshold in terms of the peak intensity of an individual laser pulse is of the order of 10^{26} W/cm².

ACKNOWLEDGMENTS

The study was funded by the Russian Science Foundation, project No. 23-72-01068.

Appendix: Transverse volume factor for Gaussian beams

Here we derive the volume factor establishing the relation between $\nu^{(\text{PWA})}$ and $\nu^{(\text{G})}$. First, we note that the Gouy phase $\psi(z)$ and the term involving $R(z)$ in Eq. (35) do not play a significant role within the LCFA calculations. This means that one can approximately assume $\tilde{g}(\chi, z, \eta) \approx f(\eta)$, where $f(\eta)$ is defined in Eq. (21). Let us represent $\nu^{(\text{G})}$ in the following form:

$$\nu^{(\text{G})} \approx \frac{1}{8\pi^3} \frac{E_0^2}{E_c^2} \int_{-\infty}^{+\infty} d\eta_- \int_{-\infty}^{+\infty} d\eta_+ \theta(f(\eta_-)f(\eta_+)) f(\eta_-) f(\eta_+) \exp \left[-\frac{\pi E_c}{E_0 \sqrt{f(\eta_-)f(\eta_+)}} \right] \Xi(\eta_+, \eta_-, E_0/(\pi E_c), \omega^2 w_0^2), \quad (\text{A.1})$$

where

$$\begin{aligned} \Xi(\eta_+, \eta_-, \mu, \beta) &= \pi\beta \int_0^{+\infty} d\chi \frac{1}{\rho^2(\eta_+ - \eta_-, \beta)} e^{-2\chi/\rho^2(\eta_+ - \eta_-, \beta)} \\ &\times \exp \left\{ -\frac{1}{\mu \sqrt{f(\eta_-)f(\eta_+)}} \left[\rho(\eta_+ - \eta_-, \beta) e^{\chi/\rho^2(\eta_+ - \eta_-, \beta)} - 1 \right] \right\}. \end{aligned} \quad (\text{A.2})$$

To explicitly indicate the β dependence of the function (32), we have also introduced

$$\rho(\eta, \beta) = \sqrt{1 + \frac{\eta^2}{\beta^2}}. \quad (\text{A.3})$$

By substituting then $e^{\chi/\rho^2} = x$, one obtains

$$\Xi(\eta_+, \eta_-, \mu, \beta) = \pi\beta \int_1^{+\infty} \frac{dx}{x^3} \exp \left\{ -\frac{1}{\mu \sqrt{f(\eta_-)f(\eta_+)}} \left[\rho(\eta_+ - \eta_-, \beta)x - 1 \right] \right\}. \quad (\text{A.4})$$

Note that if we replace the function Ξ in Eq. (A.1) with unity, the expression will yield $\nu^{(\text{PWA})}$ [see Eq. (27)]. Our goal is to find an estimate of Eq. (A.4), which is independent of η_{\pm} , so that it yields a closed-form approximate expression for $\nu^{(\text{G})}/\nu^{(\text{PWA})}$. Since the main contribution arises from the vicinity of $\eta_- = \eta_+ = 0$, we should calculate

$$\begin{aligned} \Xi(0, 0, \mu, \beta) &= \pi\beta \int_1^{+\infty} \frac{dx}{x^3} \exp \left(-\frac{x-1}{\mu} \right) = \frac{\pi\beta}{2} \left[1 - \frac{1}{\mu} - \frac{e^{1/\mu}}{\mu^2} \text{Ei}(-1/\mu) \right] \\ &= \pi\beta [\mu - 3\mu^2 + \mathcal{O}(\mu^3)]. \end{aligned} \quad (\text{A.5})$$

By substituting $\mu = E_0/(\pi E_c)$ and $\beta = (\omega w_0)^2$, we obtain Eqs. (48) and (49).

[1] F. Sauter, Über das Verhalten eines Elektrons im homogenen elektrischen Feld nach der relativistischen Theorie Diracs,

Z. Phys. **69**, 742 (1931).

- [2] H. Euler and B. Kockel, Über die Streuung von Licht an Licht nach der Diracschen Theorie, *Naturwiss.* **23**, 246 (1935).
- [3] W. Heisenberg and H. Euler, Folgerungen aus der Diracschen Theorie des Positrons, *Z. Phys.* **98**, 714 (1936).
- [4] J. Schwinger, On gauge invariance and vacuum polarization, *Phys. Rev.* **82**, 664 (1951).
- [5] A. Gonoskov, T. G. Blackburn, M. Marklund, and S. S. Bulanov, Charged particle motion and radiation in strong electromagnetic fields, *Rev. Mod. Phys.* **94**, 045001 (2022).
- [6] A. Fedotov, A. Ilderton, F. Karbstein, B. King, D. Seipt, H. Taya, and G. Torgrimsson, Advances in QED with intense background fields, *Phys. Rep.* **1010**, 1 (2023).
- [7] E. S. Fradkin, D. M. Gitman, and S. M. Shvartsman, *Quantum Electrodynamics with Unstable Vacuum* (Springer-Verlag, Berlin, 1991).
- [8] I. Bialynicki-Birula, P. Górnicki, and J. Rafelski, Phase-space structure of the Dirac vacuum, *Phys. Rev. D* **44**, 1825 (1991).
- [9] S. P. Gavrilov and D. M. Gitman, Vacuum instability in external fields, *Phys. Rev. D* **53**, 7162 (1996).
- [10] P. Zhuang and U. Heinz, Relativistic quantum transport theory for electrodynamics, *Ann. Phys.* **245**, 311 (1996).
- [11] S. Ochs and U. Heinz, Wigner functions in covariant and single-time formulations, *Ann. Phys.* **266**, 351 (1998).
- [12] S. Schmidt, D. Blaschke, G. Röpke, S. A. Smolyansky, A. V. Prozorkevich, and V. D. Toneev, A quantum kinetic equation for particle production in the Schwinger mechanism, *Int. J. Mod. Phys. E* **07**, 709 (1998).
- [13] Y. Kluger, E. Mottola, and J. M. Eisenberg, Quantum Vlasov equation and its Markov limit, *Phys. Rev. D* **58**, 125015 (1998).
- [14] V. N. Pervushin and V. V. Skokov, Kinetic description of fermion production in the oscillator representation, *Acta Phys. Polon. B* **37**, 2587 (2006).
- [15] F. Hebenstreit, R. Alkofer, and H. Gies, Schwinger pair production in space- and time-dependent electric fields: Relating the Wigner formalism to quantum kinetic theory, *Phys. Rev. D* **82**, 105026 (2010).
- [16] D. B. Blaschke, V. V. Dmitriev, G. Röpke, and S. A. Smolyansky, BBGKY kinetic approach for an $e^-e^+\gamma$ plasma created from the vacuum in a strong laser-generated electric field: The one-photon annihilation channel, *Phys. Rev. D* **84**, 085028 (2011).
- [17] A. Blinne and H. Gies, Pair production in rotating electric fields, *Phys. Rev. D* **89**, 085001 (2014).
- [18] A. Wöllert, H. Bauke, and C. H. Keitel, Spin polarized electron-positron pair production via elliptical polarized laser fields, *Phys. Rev. D* **91**, 125026 (2015).
- [19] A. Blinne and E. Strobel, Evolution of chirality in a multiphoton pair production process, *Phys. Rev. D* **93**, 025014 (2016).
- [20] I. A. Aleksandrov, G. Plunien, and V. M. Shabaev, Electron-positron pair production in external electric fields varying both in space and time, *Phys. Rev. D* **94**, 065024 (2016).
- [21] Z. L. Li, Y. J. Li, and B. S. Xie, Momentum vortices on pairs production by two counter-rotating fields, *Phys. Rev. D* **96**, 076010 (2017).
- [22] Q. Z. Lv, S. Dong, Y. T. Li, Z. M. Sheng, Q. Su, and R. Grobe, Role of the spatial inhomogeneity on the laser-induced vacuum decay, *Phys. Rev. A* **97**, 022515 (2018).
- [23] C. Schneider, G. Torgrimsson, and R. Schützhold, Discrete worldline instantons, *Phys. Rev. D* **98**, 085009 (2018).
- [24] X. G. Huang, M. Matsuo, and H. Taya, Spontaneous generation of spin current from the vacuum by strong electric fields, *Prog. Theor. Exp. Phys.* **2019**, 113B02 (2019).
- [25] X. G. Huang and H. Taya, Spin-dependent dynamically assisted Schwinger mechanism, *Phys. Rev. D* **100**, 016013 (2019).
- [26] I. A. Aleksandrov, V. V. Dmitriev, D. G. Sevostyanov, and S. A. Smolyansky, Kinetic description of vacuum e^+e^- production in strong electric fields of arbitrary polarization, *Eur. Phys. J. Spec. Top.* **229**, 3469 (2020).
- [27] I. A. Aleksandrov and C. Kohlfürst, Pair production in temporally and spatially oscillating fields, *Phys. Rev. D* **101**, 096009 (2020).
- [28] I. A. Aleksandrov, A. Kudlis, and A. I. Klochai, Kinetic theory of vacuum pair production in uniform electric fields revisited, *arXiv:2403.17204*.
- [29] G. D. Esposti and G. Torgrimsson, Momentum spectrum of Schwinger pair production in four-dimensional e-dipole fields, *Phys. Rev. D* **109**, 016013 (2024).
- [30] M. Ruf, G. R. Mocken, C. Müller, K. Z. Hatsagortsyan, and C. H. Keitel, Pair production in laser fields oscillating in space and time, *Phys. Rev. Lett.* **102**, 080402 (2009).
- [31] I. A. Aleksandrov, G. Plunien, and V. M. Shabaev, Momentum distribution of particles created in space-time-dependent colliding laser pulses, *Phys. Rev. D* **96**, 076006 (2017).
- [32] C. Kohlfürst, N. Ahmadinia, J. Oertel, and R. Schützhold, Sauter-Schwinger effect for colliding laser pulses, *Phys. Rev. Lett.* **129**, 241801 (2022).
- [33] C. Kohlfürst, Pair production in circularly polarized waves, *arXiv:2212.03180*.
- [34] I. A. Aleksandrov, G. Plunien, and V. M. Shabaev, Pulse shape effects on the electron-positron pair production in strong laser fields, *Phys. Rev. D* **95**, 056013 (2017).
- [35] O. Olugh, Z. L. Li, B. S. Xie, and R. Alkofer, Pair production in differently polarized electric fields with frequency chirps, *Phys. Rev. D* **99**, 036003 (2019).
- [36] C. Kohlfürst, Spin states in multiphoton pair production for circularly polarized light, *Phys. Rev. D* **99**, 096017 (2019).
- [37] L. N. Hu, H. H. Fan, O. Amat, S. Tang, and B. S. Xie, Spin effect induced momentum spiral and asymmetry degree in pair production, *arXiv:2402.16476*.
- [38] M. M. Majczak, K. Krajewska, J. Z. Kamiński, and A. Bechler, Scattering matrix approach to dynamical Sauter-Schwinger process: Spin- and helicity-resolved momentum distributions, *arXiv:2403.15206*.
- [39] I. A. Aleksandrov and A. Kudlis, Pair production in rotating electric fields via quantum kinetic equations: Resolving helicity states, *Phys. Rev. D* **110**, L011901 (2024).
- [40] F. V. Bunkin and I. I. Tugov, Possibility of creating electron-positron pairs in a vacuum by the focusing of laser radiation, *Dokl. Akad. Nauk SSSR* **187**, 541 (1969) [*Sov. Phys. Dokl.* **14**, 678 (1970)].
- [41] N. B. Narozhny, S. S. Bulanov, V. D. Mur, and V. S. Popov, e^+e^- -pair production by a focused laser pulse in vacuum, *Phys. Lett. A* **330**, 1 (2004).
- [42] N. B. Narozhny, S. S. Bulanov, V. D. Mur, and V. S. Popov, On e^+e^- pair production by colliding electromagnetic pulses, *JETP Lett.* **80**, 382 (2004).
- [43] S. S. Bulanov, N. B. Narozhny, V. D. Mur, and V. S. Popov, Electron-positron pair production by electromagnetic pulses, *JETP* **102**, 9 (2006).
- [44] G. V. Dunne, Q. H. Wang, H. Gies, and C. Schubert, Worldline instantons and the fluctuation prefactor, *Phys. Rev. D* **73**, 065028 (2006).
- [45] F. Hebenstreit, R. Alkofer, and H. Gies, Pair production beyond the Schwinger formula in time-dependent electric fields, *Phys. Rev. D* **78**, 061701(R) (2008).
- [46] S. S. Bulanov, V. D. Mur, N. B. Narozhny, J. Nees, and V. S. Popov, Multiple colliding electromagnetic pulses: A way to lower the threshold of e^+e^- pair production from vacuum,

- Phys. Rev. Lett. **104**, 220404 (2010).
- [47] S. P. Gavrilov and D. M. Gitman, Vacuum instability in slowly varying electric fields, Phys. Rev. D **95**, 076013 (2017).
- [48] I. A. Aleksandrov, G. Plunien, and V. M. Shabaev, Locally-constant field approximation in studies of electron-positron pair production in strong external fields, Phys. Rev. D **99**, 016020 (2019).
- [49] D. G. Sevostyanov, I. A. Aleksandrov, G. Plunien, and V. M. Shabaev, Total yield of electron-positron pairs produced from vacuum in strong electromagnetic fields: Validity of the locally constant field approximation, Phys. Rev. D **104**, 076014 (2021).
- [50] I. A. Aleksandrov, D. G. Sevostyanov, and V. M. Shabaev, Particle production in strong electromagnetic fields and local approximations, Symmetry **14**, 2444 (2022).
- [51] I. A. Aleksandrov, G. Plunien, and V. M. Shabaev, Dynamically assisted Schwinger effect beyond the spatially-uniform-field approximation, Phys. Rev. D. **97**, 116001 (2018).
- [52] Z. Peng, H. Hu, and J. Yuan, Multichannel interference in non-perturbative multiphoton pair production by gamma rays colliding, Phys. Rev. Res. **2**, 013020 (2020).
- [53] A. I. Nikishov, Pair production by a constant external field, Zh. Eksp. Teor. Fiz. **57**, 1210 (1969) [Sov. Phys. JETP **30**, 660 (1970)].
- [54] R. Schützhold, H. Gies, and G. Dunne, Dynamically assisted Schwinger mechanism, Phys. Rev. Lett. **101**, 130404 (2008).
- [55] A. Ilderton, Physics of adiabatic particle number in the Schwinger effect, Phys. Rev. D **105**, 016021 (2022).
- [56] I. A. Aleksandrov, D. G. Sevostyanov, and V. M. Shabaev, Schwinger particle production: Rapid switch off of the external field versus dynamical assistance, arXiv:2210.15626.